Journal of Alloys and Compounds, 177 (1991) 265–272
JAL 0054

Phosphorus implantation in titanium: application to calibration analysis

S. Ferdjani, D. David and G. Béranger
Université de Technologie de Compiègne, UA 849 du CNRS, BP 649, F-60206 Compiègne Cedex (France)

D. Farkas
Virginia Polytechnic Institute, Blacksburg, VA 24061 (U.S.A.)

S. Hild and E. A. Garcia*
Departamento de Ciencias de Materiales, Comisión Nacional de Energia Atómica, Buenos Aires (Argentina)

(Received June 14, 1991)

Abstract

The aim of this work is to describe some comparative analyses of implanted phosphorus in titanium by using different techniques: secondary ion mass spectroscopy, glow discharge optical spectroscopy and electron spectroscopy for chemical analysis–X-ray photoelectron spectroscopy. The amount of phosphorus was measured *vs.* depth. Mathematical simulation of the implantation process permitted the adoption of absolute units for concentration calibration. The use of these samples as standards for nuclear analysis is discussed. The main purpose of this use is to study phosphorus incorporation in titanium oxides prepared in phosphoric baths.

1. Introduction

Phosphorus analysis on the surface of metals needs well-known standards after physical and chemical preparations. To determine the overall amount of phosphorus, calibrations and concentration profile *vs.* depth are required. The choice of standard is about the most important problem in using analytical techniques with charged particle beams. In addition to the basic properties of the standard (homogeneity, durability and accuracy), fundamental parameters are very often related to two associated components: a passive matrix and the studied element. Also, it appears that the choice of studied element contributes to the analytical process, whether it is a thin film on the sample surface or a bulk distribution, depending on the preparation treatment. Thus it is necessary to know both the total amount and the depth concentration profile starting from the surface. This profile is very important because the

*Present address: Departmento de combustibles, Comisión Nacional de Energia Atómica, Buenos Aires, Argentina.

0925-8388/91/$3.50

charged particle ranges are a function of the matrix properties. Otherwise, the analytical process itself is independent of these. Here ionic implantation seems to be the appropriate technique for sample preparation. It produces near the surface (less than a few hundred nanometres) compounds such as alloys whose elaboration would have been difficult by classical metallurgical processes (melting, diffusion, etc.). This technique also has some additional interesting points: control of the particle range, which is a function of the accelerating voltage; specification of the total amount supplied to the sample, which is related to the electrical charge given by the beam; determination of the beam composition (charged particle selection technique); the possibility to implant any ion into any matrix. However, a number of secondary effects place some limitation on this technique: superficial matrix sputtering, crystalline lattice deformation, radiation damage and finally the implantation induced by diffusion [1].

We have analytically studied $^{31}P^+$ ion implantation in titanium samples by means of nuclear reaction analysis (NRA), secondary ion mass spectroscopy (SIMS), glow discharge optical spectroscopy (GDOS) and electron spectroscopy for chemical analysis–X-ray photoelectron spectroscopy (ESCA–XPS). First the experimental profiles were quantitatively compared with the theoretical ones obtained by calculation. Then they were calibrated by taking into account the total weight of implanted phosphorus. Finally the different experimental results were compared to estimate the data accuracy for definition of standards.

2. Sample preparation

Specimens of rolled kroll titanium UT35 cut from sheet of 3 mm thickness were supplied by Cezus. The impurity concentrations are given in Table 1. The mean grain size was about 30 μm. The samples were polished with SiC paper up to grade 800, then electrolytically polished in a solution of 100 ml lactic acid, 40 ml sulphuric acid and 70 ml hydrofluoric acid (constant voltage 10 V, time 6 min, temperature 0 °C) [2].

Implantations were performed with $^{31}P^+$ ions at 130 keV, simultaneously for all the samples. The beam current density was 1.5 μA cm^{-2}, with a lateral scan and a total implanted amount of 5×10^{16} atoms cm^{-2}. These

TABLE 1

Impurity concentrations (wt.%) in titanium samples

C	0.0110	Cu	0.0020
H	0.0025	Fe	0.0353
N	0.0068	Mn	<0.0050
O	0.0430	Mo	<0.0100
Al	0.0010	Si	<0.0300
V	0.0074	Sn	<0.0100

values reduced the radiation damage and sputtering phenomena to a minimum, while the phosphorus concentration was higher than the detection limit of the analytical techniques used.

3. Concentration profile determination

The experimental profiles were obtained by means of SIMS and GDOS, with some complementation by ESCA–XPS.

3.1. SIMS analysis

The phosphorus profile was obtained with an O_2^+ primary ion beam (10 keV, 60 nA), a lateral scan reducing the effects of cratering. The emitted PO_2^- ions were analysed taking into account the background noise (possible interference with $^{47}TiO^-$ ions, whose mass value 63 is the same) (Fig. 1).

Up to a depth of 40 nm the profile shows a deformation, perhaps related to the oxide layer always present on metallic surfaces [3]. Probably the sputtering rate is different for this oxide and the metal itself, but since the difference is unknown, we neglect it. If we assume in a first approach that the profile is fitted by a gaussian function, the parameters of this are R_p (mean value of the variable, giving the peak abscissa of the curve) and the standard deviation ΔR_p. Then the mid-height width is $l_{1/2} = 2.36\Delta R_p$. Physically, R_p is the mean range value of the implanted ions perpendicular to the surface of the sample; ΔR_p is the straggling or energy scattering with depth.

The implanted ion concentration $n(x)$ at a depth x after a time t is given by

$$n(x) = \frac{\Phi t}{2\pi\Delta R_p} \exp\left(- \frac{x - R_p)^2}{2(\Delta R_p)^2} \right)$$

where Φ (atoms cm^{-2} s^{-1}) is the implanted flux.

In an experimental way the Fig. 1 profile allows us to determine the following values: $R_p = 95$ nm, $l_{1/2} = 100$ nm and $\Delta R_p = 43$ nm.

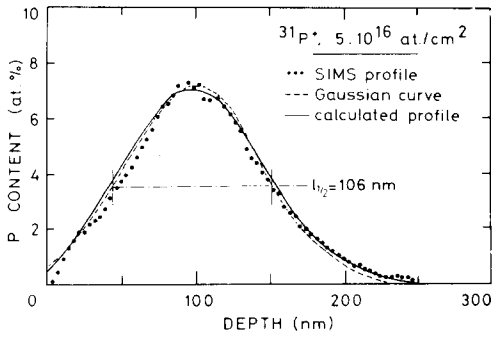

Fig. 1. SIMS profile and calculated curve.

The calibration *vs.* depth was performed by mechanical processes on titanium samples with the same ionic sputtering but without any implantation. In fact, the indetermination in these depth values is rather high, about 20–25 nm.

3.2. GDOS analysis

We have measured the phosphorus profile for a 700 V discharge voltage of duration 15 s. The sputtering rate was about 23 nm s^{-1}, the depth calibration resulting from the SIMS analyses [4]. This profile compares reasonably with the SIMS one up to about 130 nm. At higher depth values it broadens out (Fig. 2). This broadening is a function of the discharge voltage, which we could see by an analysis performed at 800 V. To all appearances it is related to the analytical process and not to the phosphorus amount itself.

3.3. ESCA–XPS analysis

The previous analyses were complemented by an ESCA–XPS analysis performed on a single sample. The apparatus used was a VG spectrometer with a magnesium anticathode under a vacuum of 10^{-8} Torr. The ionic sputtering was performed by means of an Ar^+ beam at a mean rate of about 0.2 nm mA^{-1}. Under these conditions the depth values estimated were rather poor ($\pm 25\%$). The peak of the curve appears at a depth value of about 120 nm and, because of the indetermination, was fitted to the same value as the previous ones obtained by SIMS and GDOS (Fig. 3). This fitting is perhaps an extreme simplification. During the ionic sputtering, a shift of the peak may be induced by secondary effects such as radiation-induced segregation and differential sputtering rate. The sputtering rate is thus an essential parameter for the understanding of these phenomena [5, 6]. Because of the much lower concentrations for low and high depth values, the analysis did not supply the complete profile. There is always a dissymmetry, with a broadening after the peak of the curve. This effect could be due to the fact that the incident angle used for the argon sputtering induced re-implanted

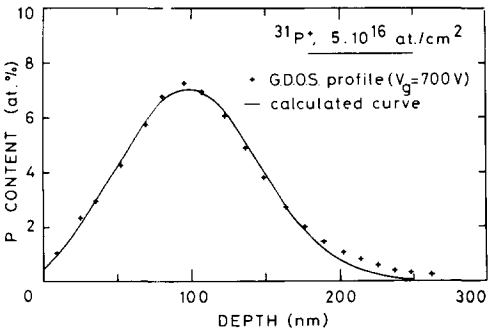

Fig. 2. GDOS profile and calculated curve.

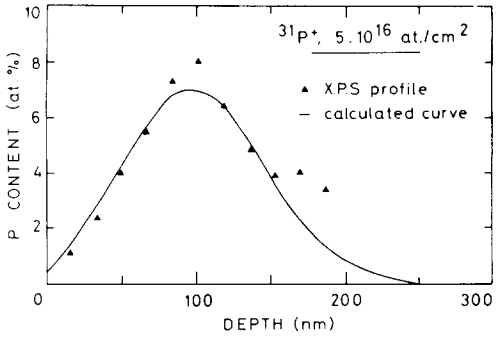

Fig. 3. ESCA–XPS profile and calculated curve.

TABLE 2

Phosphorus binding energies for selected compounds (from *Handbook of X-Ray Photoelectron Spectroscopy*, Perkin–Elmer Corporation)

Compound	2p binding energy (eV)
CrP	128.4
MnP	128.9
GaP	128.9
BP	129.1
P	129.6
KH_2PO_4	133.5
$POBr_3$	134.0
$(NaPO_3)_3$	133.6
$NaPO_3$	134.1
P_2O_5	135.0

phosphorus. For this reason the higher concentration value could be shifted to increasing depth.

The energy of the phosphorus peak was 129.0 ± 0.2 eV. This value is in agreement with those of the P_2 peaks observed for anodic oxides containing additional phosphorus [7]. It corresponds also to the P^0 phosphorus value, but some phosphides such as MnP and GaP have the same one. Insufficient data are available on phosphides and atomic phosphorus in titanium in order to discriminate between these peaks on an energy scale (Table 2). Nevertheless, this value would be in good agreement with atomic phosphorus on interstitial sites.

4. Theoretical simulation of the implantation process

Because the fitting by a gaussian function is not very good, the phosphorous implantation process for a polycrystalline material was simulated by a mathematical theory according to ref. 8. Starting from a gaussian distribution *vs.*

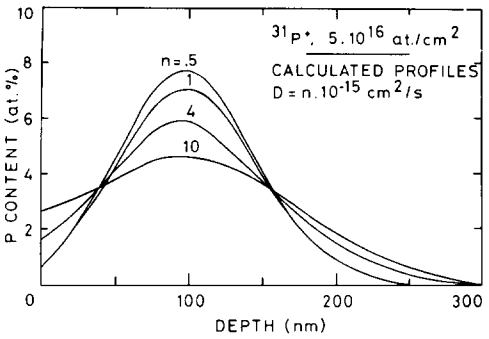

Fig. 4. Calculated profiles *vs.* diffusion coefficient value.

depth, which is a function of the implantation energy, the theory takes into account the secondary effects of diffusion, collisional mixing, sputtering and crystal lattice deformation. The last two effects are equivalent to a new reference system, but we can neglect them under our experimental conditions since the total phosphorus amount is small [9].

However, we cannot neglect the diffusion effect, as shown by the calculated profiles for different values of the diffusion coefficient D in Fig. 4. First we have fitted these calculated profiles with the experimental ones measured by means of SIMS and GDOS. The single parameter is then D, without quantitative units for the concentration scale. Nevertheless, the best fit is given for $D = 1 \times 10^{-15}$ cm^2 s^{-1}, with a sputtering ratio value equal to 2. According to Dearnaley *et al.*, the diffusion coefficient value is in this range for an implanted flux between 1×10^{13} and 10×10^{13} ions s^{-1} cm^{-2}, which is very close to our experimental conditions [1]. In contrast, for all D values it is impossible to fit a calculated profile to the ESCA–XPS one, because this latter is dissymmetrical.

5. Application to calibration analysis

The first stage being the fitting to the profile shape, we have in a second step calculated absolute concentration values for the SIMS and GDOS profiles. The fundamental parameter was the total amount of implanted phosphorus, *i.e.* the calculated profile integral.

5.1. SIMS and GDOS analyses

The secondary ionic emission may be calibrated if the relationship between the signal–depth curve and the phosphorus profile is known. The easiest case would then be a constant signal–concentration ratio, which describes our example. The other condition is a constant value for the sputtering rate (homogeneous material with low impurity concentration). Then the signal–depth curve may be fitted to the calculated profile, which gives it absolute value. The maximum value is for a phosphorus amount equal to 7.3 at.%

(Fig. 1). We have performed the same process on the GDOS profiles (Fig. 2).

5.2. NRA

NRA gives absolute results with good accuracy for both the concentration profile and its integral. Although it remains a comparative technique, it gives us a more accurate comparison between the samples and some standards. However, when the purpose is the calibration of these standards, NRA cannot supply absolute measurements in this case (Fig. 5). We used the $^{31}P(p, \alpha)^{28}Si$ reaction with incident protons of 1880 keV and detection at an angle of 150°. Under these conditions the differential cross-section has a resonance peak (peak level 21 mb/st, mid-height width 23 keV) [10]. The emitted α particles have a low energy, so that it is not possible to use a filter for stopping the backscattered protons. Thus the incident beam intensity must be small (a few tens of nanoamperes per square centimetre), a condition which does not completely eliminate noise. These experimental conditions are not convenient [11].

However, profiles measurements are still possible using a simulation calculation and the fitting of the calculated spectra to the experimental ones [12]. Here we have only performed homogeneity and reproducibility controls.

With a sample size of 27×14 mm^2, 3 mm between two measuring points and 1 mm diameter for each point, the scattering of results is $\pm 1.25\%$, including the nuclear statistical contribution. Thus the homogeneity is very good.

However, the phosphorus amount decreases by about 11% during analysis for a 1000 μC incident beam. This value is reached in a cumulative measuring time of about 4–5 h. Since the beam current is very small and reasonable accuracy requires about 30 min for each analysis, we cannot neglect this decrease in phosphorus amount. However, it is lower than that for chemical samples, which reaches about 85% for a 15 μC beam charge [13]. These

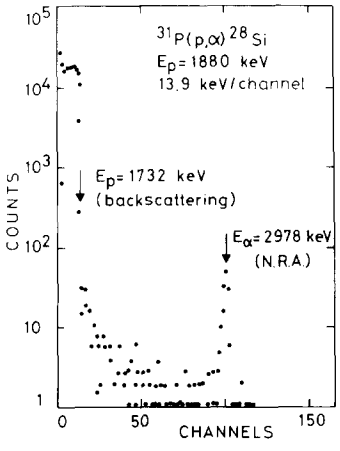

Fig. 5. NRA spectrum for the $^{31}P(p, \alpha)^{28}Si$ nuclear reaction [13].

NRA standards have been used for studying phosphorus incorporation in anodic oxide thin films grown in phosphoric baths [7].

6. Conclusions

Implanted profiles may be observed by SIMS with good accuracy. Taking into account the total amount of implanted ions, it is easy to have well-known reference samples with absolute concentration values *vs.* depth.

In contrast, the GDOS results are dependent on the experimental conditions and the ESCA–XPS sensitivity is not sufficient for profiling under our experimental conditions.

A better fit of the experimental profiles is possible using a simulation calculation for the implantation process, taking into account secondary effects, which increase with increasing amount of implantation. Then the samples are very suitable for calibrating NRA processes using simulation treatment for experimental data up to a few micrometres depth; this is better than etching but it is necessary to have concentration and shape standards.

Acknowledgments

The authors are grateful to F. Maurice (CEN, Saclay), R. Berneron and D. Loison (IRSID, Usinor Sacilor, St Germain-en-Laye), J. Chaumont (Paris XI University) and A. Vejux (Compiègne University) for their help.

This work was supported by the CNRS (GR 86 and UA 849).

References

1 G. Dearnaley, J. H. Freeman, R. S. Nelson and J. Stephen, *Ion Implantation*, North-Holland, Amsterdam, 1973, p. 228.
2 D. David, P. Cremery, C. Coddet and G. Béranger, *J. Less-Common Met.*, *69* (1980) 81.
3 G. Béranger, D. David, E. A. Garcia and X. Lucas, *Rev. Phys. Appl.*, *10* (1975) 87.
4 R. Berneron, *Spectrochim. Acta B*, *33* (1978) 665.
5 N. Q. Lam, *Surf. Interface Anal.*, *12* (1988) 65.
6 E. Darque-Ceretti and M. Aucouturier, *Nucl. Inst. Methods in Phys. Res.*, *B52* (1990) 79.
7 S. Ferdjani, D. David and G. Béranger, *Microsc., Microanal., Microstruct.*, *1* (4) (1990) 275.
8 D. Farkas, I. L. Singer and M. Rangaswamy, *J. Appl. Phys.*, *57* (1985) 1114.
9 S. Ferdjani, *Thesis*, Compiègne, 1986.
10 G. Guernet, E. Ligeon, N. Longequeue, Tsan Ung Chan and J. P. Longequeue, *J. Phys. (Paris)*, *29* (1968) 9.
11 R. Caplain, S. Ferdjani, D. David and G. Béranger, *Surf. Sci.*, *162* (1985) 865.
12 D. David, G. Béranger and E. A. Garcia, *J. Electrochem. Soc.*, *130* (6) (1983) 1423.
13 E. Ligeon, M. Bruel, A. Bontemps, G. Chambert and J. Monnier, *J. Radioanal. Chem.*, *16* (1973) 537.